



The influence of the ratio between the wire and process velocities on the wetting process during laser brazing

Thorsten Mattulat¹ · Peer Woizeschke¹

Received: 8 June 2020 / Accepted: 4 August 2020 / Published online: 17 August 2020
© The Author(s) 2020

Abstract

Laser brazing is used in automotive production for the joining of car body parts with customer-visible seams, whereby the highest optical seam quality is demanded. During the wetting process, a constriction formation can occur within the molten brazing material, which subsequently collapses; this induces a stepwise progression of the wetting front, thereby decreasing the optical seam quality. The aim of this study is to investigate the influence of the wire and process velocities on this constriction formation. For this purpose, high-speed recordings of the process zone are performed during laser brazing and then evaluated concerning the wetting process. The results show that the constriction formation depends on the relationship between the process velocity and the process direction component of the wire velocity. The constriction formation only occurs when the process velocity exceeds the parallel-oriented component of the wire velocity. This constriction formation is unstable and collapses repeatedly. In this study, increasing velocity differences stabilizes the constriction existence. This stabilization correlates with a uniform wetting process and a reduced frequency of the occurrence of blowout events, probably due to improved outgassing of zinc bubbles from the melt pool.

Keywords Joining · Laser material processing · Laser brazing · Wetting · Process monitoring

1 Introduction

Laser material processing is a technology that is used for many applications in the production process of the automotive industry [1]. Here, laser brazing is used for the joining of car body parts [2], which are by default zinc-coated for corrosion protection [3]. Standard applications are a connection between the two-part trunk lid [4] or the connection of the roof and side panel [5]. The brazed seams remain directly visible (except for painting) to the customers [6], and hence, the highest optical quality standards are demanded for these seams [7]. This includes, for example, straight seam edges, a smooth seam surface, and the absence of adherent spatter or pores and holes [8].

To ensure optical seam quality, the wetting process in laser brazing is of major importance [9]. As an example, the mechanism of pore formation is described by Frank et al. as the formation of constrictions in the area of the wetting front as a consequence of a temporary interruption of the wire feed [10]. However, such a constriction formation is not only observed during disturbed process behavior. Grimm and Schmidt first reported these constrictions for a sound brazing process with constant process parameters, occurring at a frequency of approx. 30 Hz and inducing a stepwise progression of the wetting process [11]. They assume that the formation of constrictions depends on effects that are connected to the process velocity. This stepwise progression of the wetting front was also reported by Reimann, who found a wetting frequency of 39 Hz [12], and by Heitmanek et al., who determined a frequency of 42 Hz [13]. Further evaluation of the formation of constrictions was carried out by Heuberger et al. [14], who detected the constriction formation in a constant brazing process using high-speed recordings from the top view. Here, the length of the constrictions increased with increasing process velocity. At a critical length, the constrictions spontaneously collapsed and induced an abrupt propagation of the wetting process.

Electronic supplementary material The online version of this article (<https://doi.org/10.1007/s11740-020-00978-5>) contains supplementary material, which is available to authorized users.

✉ Thorsten Mattulat
mattulat@bias.de

¹ BIAS - Bremer Institut für angewandte Strahltechnik GmbH, Klagenfurter Str. 5, 28359 Bremen, Germany

This abrupt collapse of the constrictions has been found to be a reason for defects concerning the optical seam quality, such as the formation of notches at the seam edges. Furthermore the collapse of constrictions was found as a cause for wavy seam edges due to an change in seam width during the abrupt progress of the wetting fronts [15].

Another factor influencing the wetting process and the optical seam quality is the zinc coating of the base material. Gatzen et al. showed that the molten zinc layer can merge with the melt pool during the brazing process [16]. The zinc, which has a comparatively low boiling temperature of 907 °C [17], can hereby evaporate during the process and create melt pool surface instabilities [14] and openings in the melt pool in combination with spatter formation [18].

2 Aim

As mentioned above, a constriction formation with subsequent collapse during laser brazing can induce an unsteadily progressing wetting process and lead to seam defects like pores, notches or wavy seam edges. However, it is currently not known what dominant mechanisms are responsible for this constriction formation. A possible explanation is that it originates from an unsuitable relationship between the feed rate of the filler wire and the process velocity. Therefore, this study examines the hypothesis that the formation of constrictions is induced by a mismatch in the relative velocity between the process movement and the velocity component of the wire feed oriented parallel to the process direction. This velocity difference is illustrated in Fig. 1.

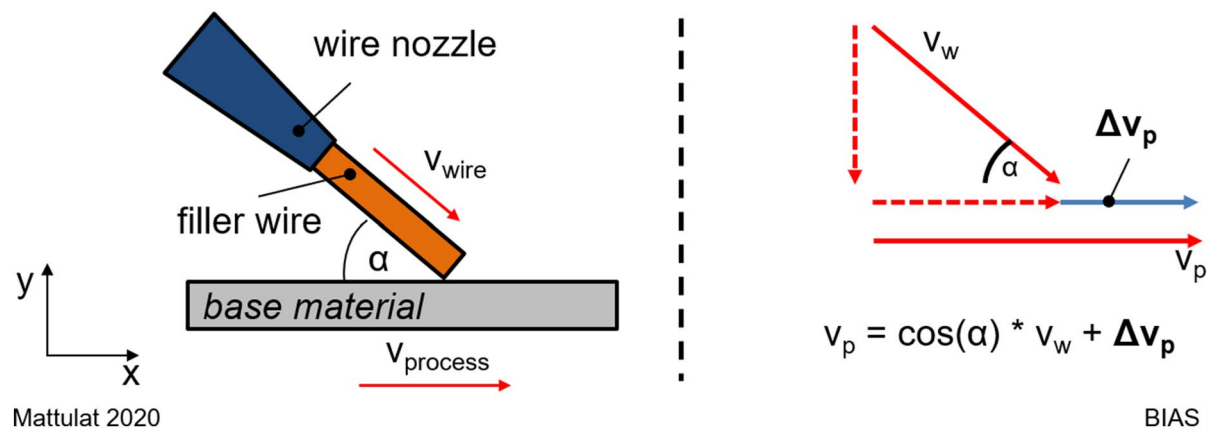


Fig. 1 Schematic sketch of the brazing process in the case of a moving workpiece (left) and the velocity components (right): wire velocity v_w , process velocity v_p and velocity difference Δv_p

Table 1 Chemical composition of the filler material used in wt%

Si	Mn	Fe	Zn	Sn	Pb	Al	Cu
2.88	0.84	0.009	0.005	0.002	0.001	0.001	Bal

3 Experimental

3.1 Materials

The base material for the brazing experiments was the electrolytically galvanized steel DC06 + ZE75/75. The dimensions of the base material sheets were 150 mm in length, 50 mm in width, and 0.75 mm in thickness. The filler wire had a diameter of 1.2 mm and the material was CuSi3Mn1, which has a melting range of 965°–1035 °C and whose composition is shown in Table 1. The materials used are common in the industrial application of laser brazing in automotive body construction.

3.2 Brazing setup

A Trumpf TruDisk 12002 disk laser with a wavelength of 1030 nm was used as a laser beam source. The beam was transferred by a fiber with a core diameter of 0.6 mm to a Scansonic ALO3 brazing optic, which is commonly used for brazing in automotive production. In the brazing optic, an imaging ratio of 4:1 was realized, resulting in a nominal focus diameter of 2.4 mm. The focal plane of the laser beam was set on the surface of the workpiece in order to achieve a top-hat intensity profile at this position. The movement of the additional axes of the brazing optic, which are used in industrial production for tactile seam tracking, was blocked during this study. The wire nozzle, which is part of the brazing optic, had an inclination angle of 45° relative to the horizontal axis of the optic. To avoid back reflections from the

workpiece, the brazing optic was mounted to the processing station with an angle of 5° to the vertical, meaning the total wire angle relative to the process direction was 40°. The wire stick-out and the impinging point of the filler wire relative to the laser spot were calibrated using a setup spike provided by the optic manufacturer. The stick-out was set to 8 mm and the impinging point of the filler wire was positioned with a shift of 0.5 mm to the spot center in the direction of the wire nozzle. For wire feeding, a High-Dynamic-Drive (HDD) system with a push–pull configuration by Dinse was used. In contrast to the standard in industrial application, the process movement was not realized by moving the brazing optic but rather by moving the base material in the opposite direction; cf. Fig. 1. This enabled a permanent process monitoring of the wetting process by a stationary camera, whereby the position of the wetting process relative to the camera did not change. Using this setup, bead-on-plate experiments with seam lengths of 120 mm were performed. The experimental setup is illustrated in Fig. 2.

3.3 Process monitoring

The wetting process during the brazing experiments was recorded using a stationary high-speed camera (Vision Research Phantom VEO 410L), which was positioned orthogonal to the process direction and with a vertical inclination of 5° (cf. Fig. 2). A macro-objective in combination with an extension bellows was used to achieve a high magnification of the process zone. In order to eliminate any disturbing influences of the brazing process radiation, a Cavitax

laser was recorded by the camera. The parameters used for the recordings are given in Table 2.

3.4 Variation of the velocity difference Δv_p

The experiments of this study included a variation of the velocity difference Δv_p referring to the exemplary brazing setup given in Fig. 1. According to Eq. 1, where v_p is the process velocity, v_w is the wire velocity, and α is the constant inclination angle of the wire relative to the process direction, the velocity difference can be adjusted by changing the ratio between the process and wire velocity. Here, a positive value of Δv_p means a higher process velocity compared to the component of the wire velocity oriented parallel to the process direction.

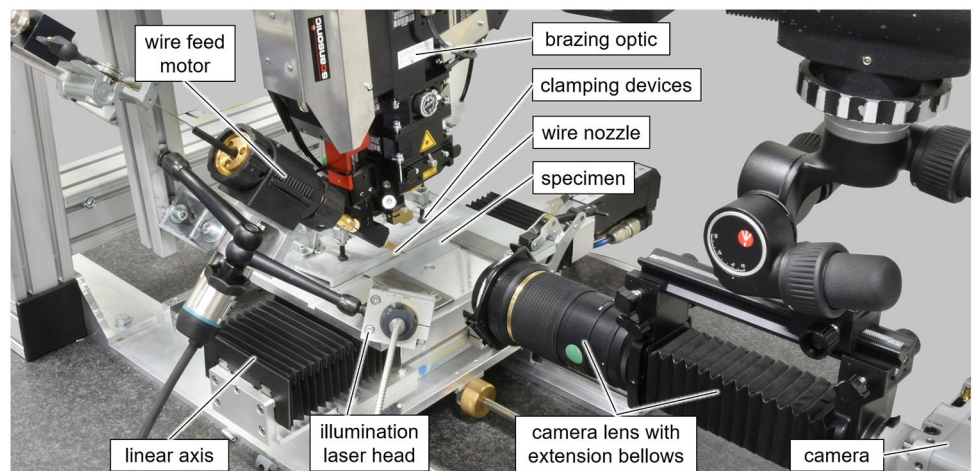
$$v_p = \cos(\alpha) * v_w + \Delta v_p \tag{1}$$

In the first instance, the wire velocity was set to a constant value of 50 mm/s and the velocity difference Δv_p was varied from – 20 up to 90 mm/s. Here it has to be mentioned, that

Table 2 Parameters used for the high-speed recordings of the process

Sample rate (Hz)	Exposure time (μ s)	Resolution (px * px)	Total recording time (s)	Illumination wavelength (nm)	Illumination pulse duration (μ s)
10,000	10 μ s	800 * 512	1	810	1.33

Fig. 2 Experimental setup for brazing experiments



Mattulat 2020

BIAS ID 200483

Cavilux HF illumination laser system was used, which illuminated the process zone with radiation of a central wavelength of 810 nm. By mounting an 810 ± 12 nm FWHM (Full Width at Half Maximum) bandpass filter in front of the camera, only the reflected radiation of the illumination

a change in Δv_p also means a change in the seam volume due to a change in amount of filler wire per brazing length. Furthermore, experiments with $\Delta v_p = 0$ for varied values of the wire velocity, starting from 25 up to 100 mm/s, were conducted. In all experiments, the energy per wire volume

was kept constant with a value of 40 J/mm^3 . Each experiment was carried out three times.

3.5 Evaluation of the wetting front (and wire) movement

The experiments described in the previous section were evaluated concerning the movement of the wetting fronts. To visualize the wetting front behavior, streak images were created from the high-speed recordings. For the creation of streak images, one row in the recording was selected and extracted from each frame of the video, and then each was assembled one below the other in chronological order. When choosing a row in which the wetting process was visible, the corresponding streak image revealed the time-dependent movement of the wetting front. Due to the illumination by the illumination-laser system, the recorded image depended on the reflection of the radiation in the process zone. Hereby, the wetting fronts directly reflected the radiation into the camera, resulting in a local brightness maximum in the recordings. By tracing the right border of the brightness maximum, the wetting front movement could be extracted from the streak images (cf. Fig. 3). 3000 frames (0.3 s) were selected from the middle of the recording per experiment to eliminate side effects at the process start and end. Considering the movement of the wetting front as an oscillating process (as repeatedly assumed in the literature), the amplitude of the wetting front movement was determined. For this, each streak image was divided into ten equally sized parts and the distance between the first and the second visible local maxima was measured for each part. Values for the amplitude of the oscillation are calculated by dividing the measured values by two.

The generation of streak images is also used to illustrate the movement of the filler wire over time. For this, a row where the lower border of the filler wire is visible and the

wetting process is not visible (to prevent the lower edge from being covered by the wetting process) is selected (cf. Fig. 3).

3.6 Evaluation of the wetting front length

The value for the length of the wetting front is defined in this study as the distance between the right border of the wetting front and the impinging point of the lower border of the filler wire on the base material in the process recordings. This method allows the measurement independent of whether a constriction in the area of the wetting fronts is present or not. The rightmost measured values for each of the ten parts from the streak images (cf. previous section) were used to determine the position of the right border from the process recordings. The impinging point of the filler wire was determined from ten equally distributed frames from each process recording. Here, the intersection between the lower wire border with a line, defined by the projection of the wire axis on the base material, was considered, as illustrated in Fig. 4.

3.7 Evaluation of the blowout event density

Blowout events in the region of the wetting fronts, characterized by a disturbance of the melt pool surface and an explosive melt ejection, were visible in the streak images as horizontal lines because they only appeared in a short time frame (cf. Fig. 5). To determine a value for the density of these blowout events for the different experiments, the horizontal lines in the streak image were counted and this number was divided by the respective process velocity. Thereby, one value for the blowout event density was calculated for each experiment.

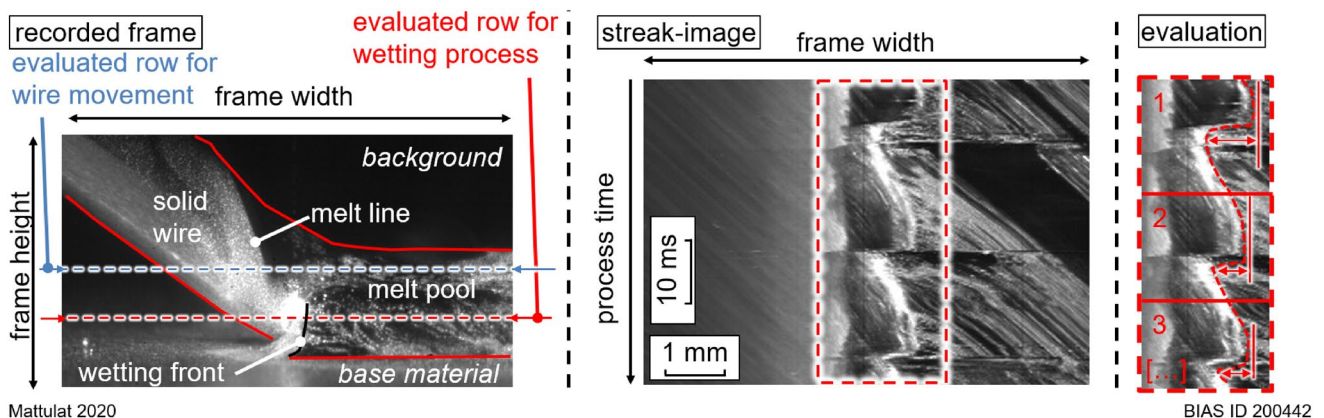
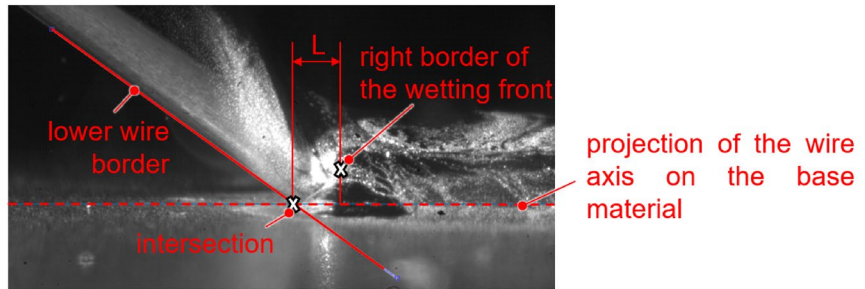


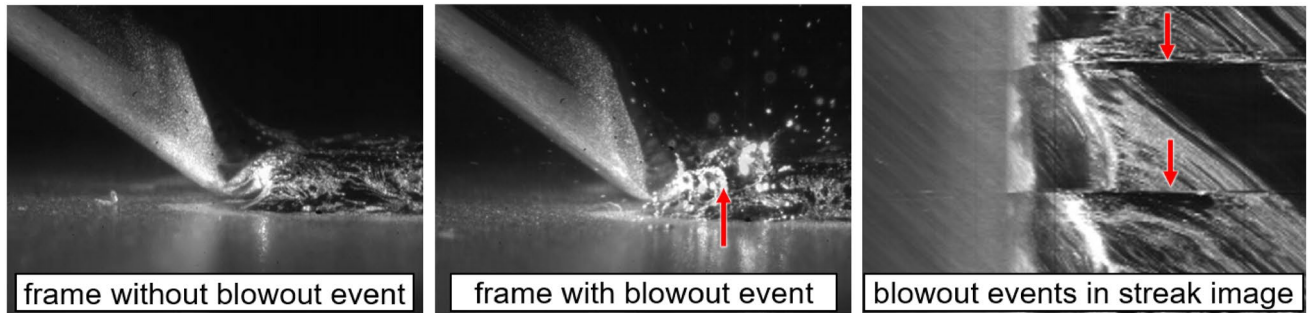
Fig. 3 Classification of the process recordings and evaluation of the streak images

Fig. 4 Definition of a value for the wetting front length



Mattulat 2020

BIAS ID 200443



Mattulat 2020

BIAS ID 200444

Fig. 5 Exemplary frames with and without blowout events in the recorded frames and the appearance of blowout events in the streak images

4 Results

In Fig. 6 the wetting process is visualized by the streak images for different values of Δv_p , starting with a velocity difference of 0 mm/s and decreasing the value, resulting in a higher wire velocity in the process direction relative to the process velocity. The results only show small fluctuations in the movement of the wetting progress for varied Δv_p , except for the lowest investigated value of -20 mm/s, where irregular variations of the wetting front position occur.

Considering the same type of presentation for velocity differences from 0 to 90 mm/s, whereby the process velocity was higher than the component of the wire velocity in the process direction, major changes in the wetting process could be observed (cf. Fig. 7). Compared to the initial state without a velocity difference, the variation of the wetting front position increased in its amplitude up to $\Delta v_p = 30$ mm/s. At a further increase in the velocity difference, the amplitude of the variation of the wetting front position decreased again. Besides the decrease in amplitude, an increase in the frequency of the wetting front movement could also be observed.

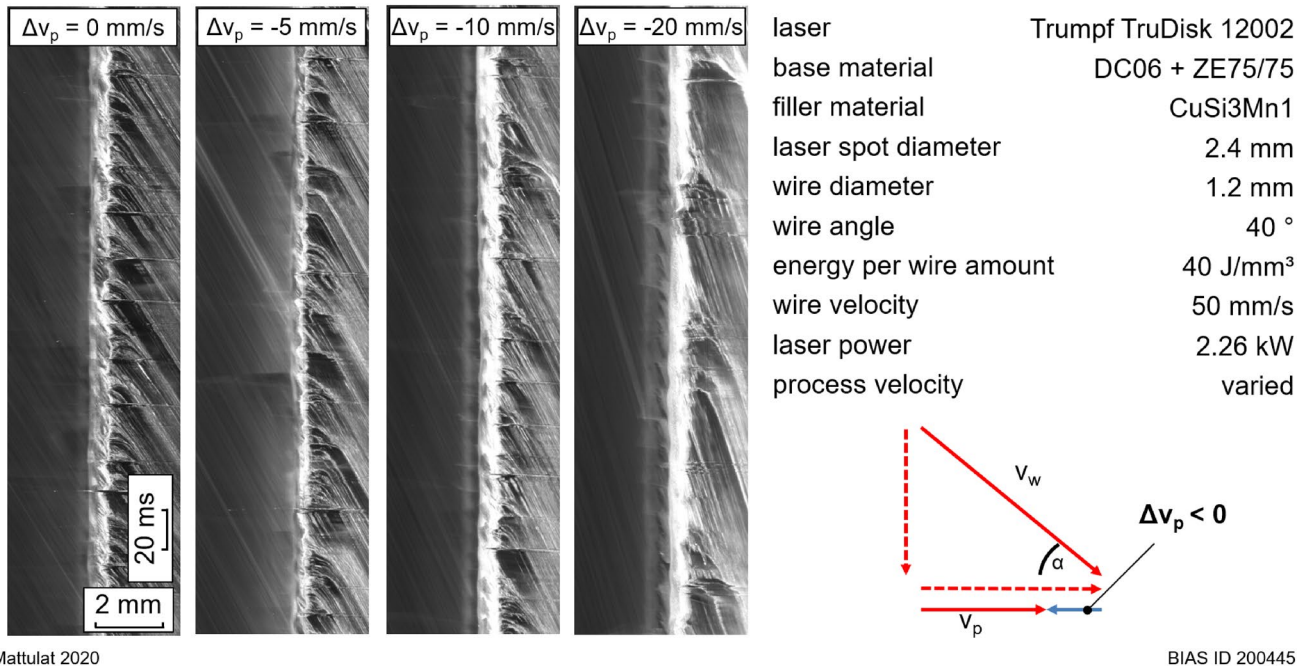
The measurements of the amplitude of the wetting front movement are displayed in Fig. 8. At $\Delta v_p = 0$ mm/s, a wetting front amplitude of 0.06 ± 0.02 mm was obtained. With

increasing velocity difference, the amplitude also increased up to a value of 0.13 ± 0.03 mm for $\Delta v_p = 30$ mm/s. The lowest average value of 0.05 ± 0.03 mm was determined for a velocity difference of -10 mm/s. Comparing the measuring results of the wetting front amplitude for $\Delta v_p = 0$ mm/s with the highest investigated values for $\Delta v_p (\geq 60$ mm/s), the average values were at the same level.

Besides the aforementioned movement of the wetting process, the shape of the wetting fronts was also further analyzed, as shown in Fig. 9. Without a velocity difference and with negative values for Δv_p , the wetting fronts showed a steep angle, connecting the melt pool with the base material. A change in shape was detected when a positive velocity difference was present. Here, the formation of a constriction between the melting filler wire and the wetted base material was present. A further increase in the velocity difference resulted in an increased length of these constrictions.

Streak images, which illustrate the position of the filler wire during the brazing process for varied values of Δv_p , are given in Fig. 10. For all investigated experiments, no displacement of the wire position during the process nor an oscillating or discontinuous behavior were detected.

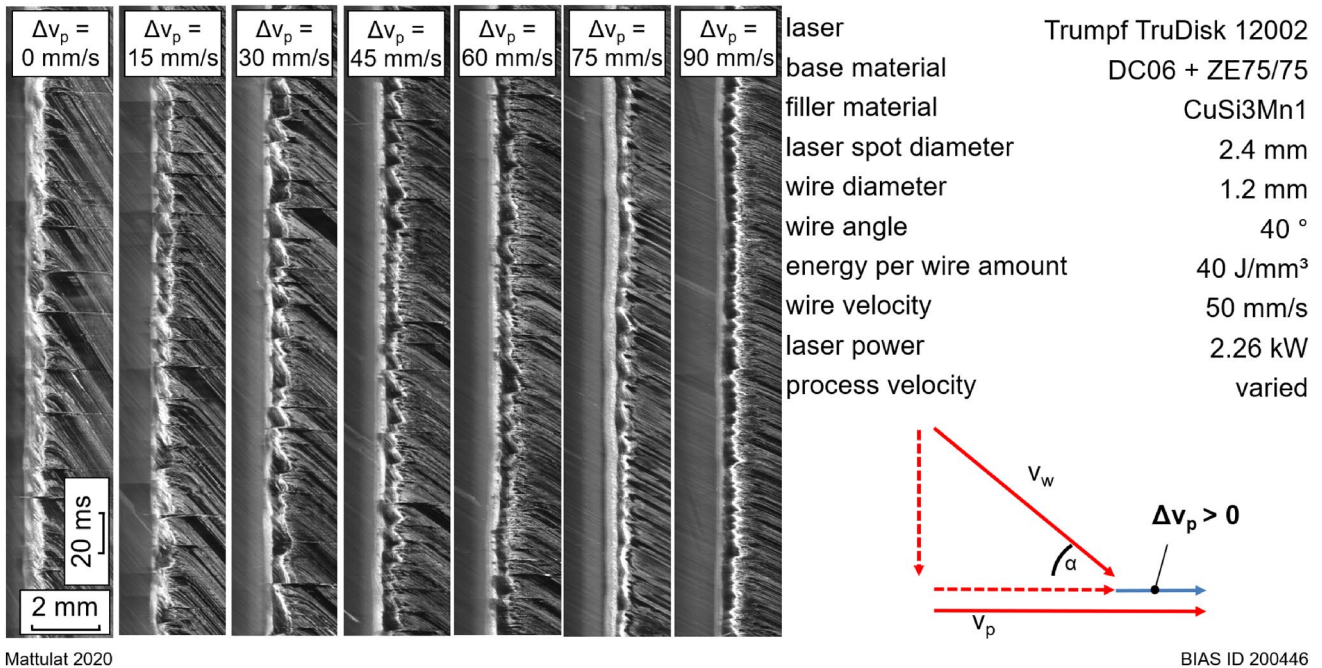
The measuring results of the constriction length are presented in Fig. 11. The constriction length increased with increasing Δv_p until a value of $\Delta v_p = 30$ mm/s. For higher values for Δv_p , no further steady increase can be observed.



Mattulat 2020

BIAS ID 200445

Fig. 6 Comparison of the wetting process by the streak images for varied $\Delta v_p \leq 0$



Mattulat 2020

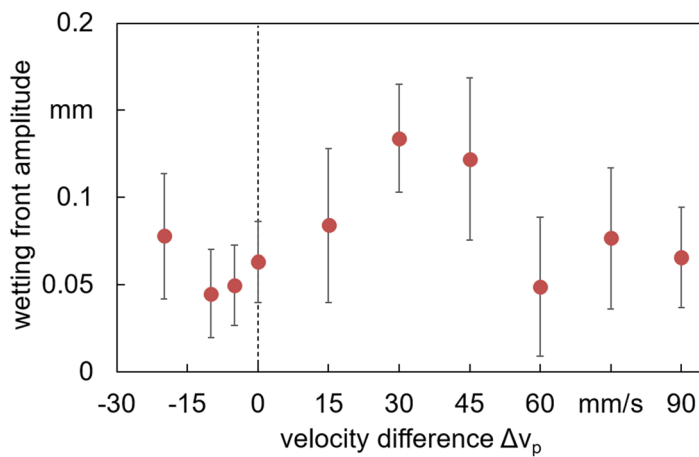
BIAS ID 200446

Fig. 7 Comparison of the wetting process by the streak images for varied $\Delta v_p \geq 0$

The highest constriction length was found for the highest investigated velocity difference of 90 mm/s with a value of $0.60 \text{ mm} \pm 0.05 \text{ mm}$. Even though no constriction formation could be detected for values of $\Delta v_p \leq 0$, a shortening

of the wetting front at decreasing velocity differences was determined.

The results of the evaluation concerning the blowout event density from the area of the wetting fronts are presented in Fig. 12; the median value and the maximum and

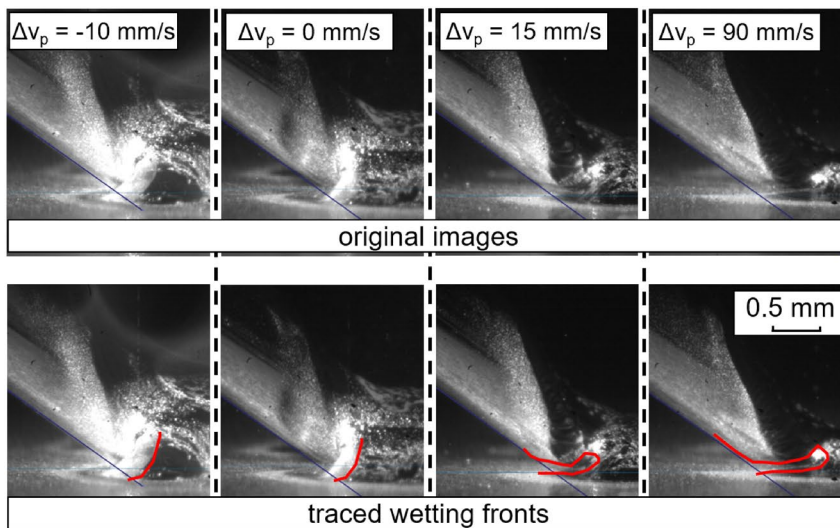


laser	Trumpf TruDisk 12002
base material	DC06 + ZE75/75
filler material	CuSi3Mn1
laser spot diameter	2.4 mm
wire diameter	1.2 mm
wire angle	40 °
energy per wire amount	40 J/mm ³
wire velocity	50 mm/s
laser power	2.26 kW
process velocity	varied

Mattulat 2020

BIAS ID 200447

Fig. 8 Results of the measurement of the wetting front amplitude for varied Δv_p



laser	Trumpf TruDisk 12002
base material	DC06 + ZE75/75
filler material	CuSi3Mn1
laser spot diameter	2.4 mm
wire diameter	1.2 mm
wire angle	40 °
energy per wire amount	40 J/mm ³
wire velocity	50 mm/s
laser power	2.26 kW
process velocity	varied

Mattulat 2020

BIAS ID 200448

Fig. 9 Shapes of the wetting fronts for varied Δv_p

minimum deviations are given. The density tends to decrease with increasing velocity difference Δv_p . At the highest investigated Δv_p , the value of $0.08 + 0.03 \text{ mm}^{-1}$ indicates that nearly no blowout events occurred.

The streak images for experiments with different wire and process velocities are presented in Fig. 13. The process velocity v_p was adapted for four different wire velocities v_w to obtain the constant relation of $\Delta v_p = 0$ between v_w and Δv_p . Here, it can be seen that the variation of the wetting fronts was at the same level for the wire velocities of 50 mm/s, 75 mm/s, and 100 mm/s and that no significant differences in the wetting process could be observed. An exception was the experiment with the lowest investigated wire velocity of 25 mm/s, as here, apart from an

otherwise constant wetting process, occasional changes of the wetting front position could be observed.

Experiments with different values for Δv_p and v_w were compared concerning the process velocity to separate the effects of a velocity difference Δv_p from the effects of the absolute process velocity v_p (cf. Fig. 14). Here, it can be seen that the lowest amplitude was obtained for $\Delta v_p = 0 \text{ mm/s}$ (purple circles).

A direct comparison of the process recordings of the abovementioned experiments with comparable absolute process velocities in the range of 80 mm/s for different values of Δv_p is presented in Fig. 15. Here, it can be seen that in the case of $\Delta v_p = 45 \text{ mm/s}$, a constriction formation

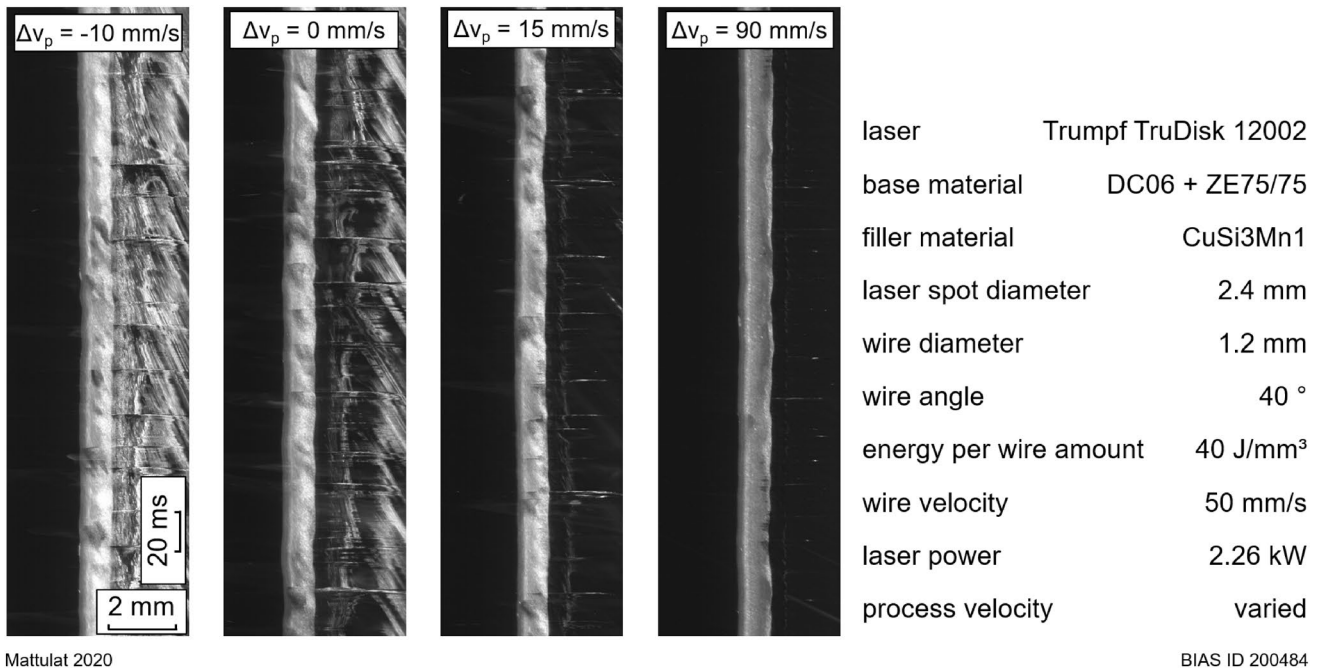


Fig. 10 Horizontal movement of the filler wire, illustrated by streak images for varied values of Δv_p . Note: The movement of the left border of the bright area in the streak image correspond to the movement of the lower wire border

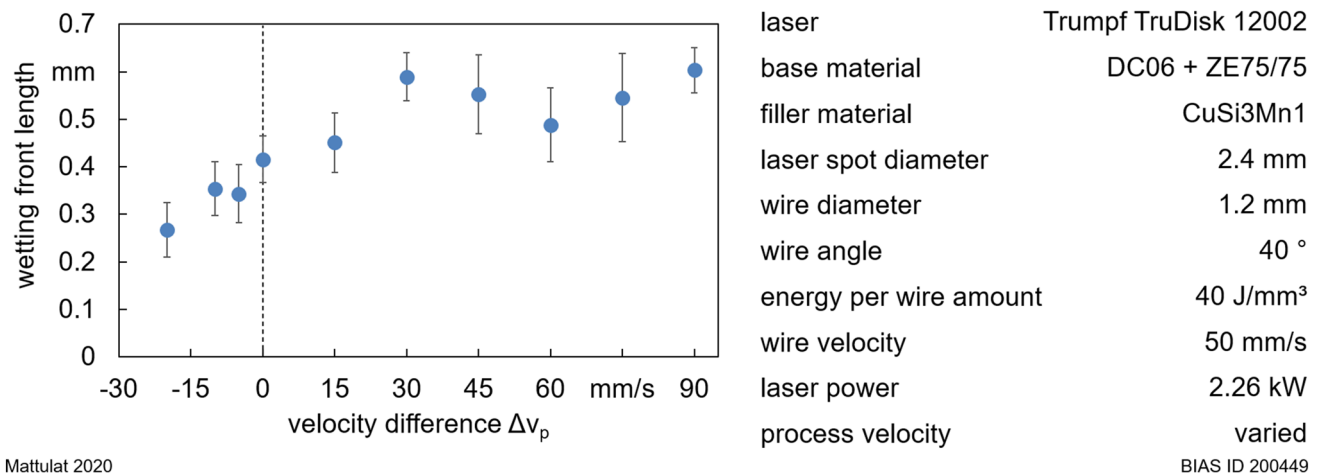
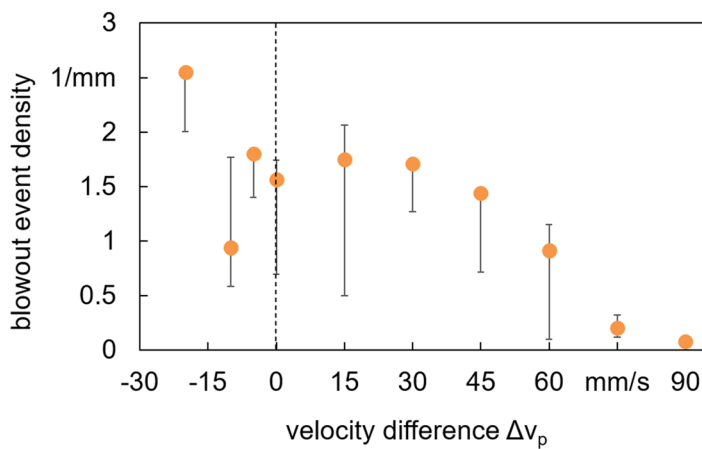


Fig. 11 Measurement results for the wetting front length at different values of Δv_p , whereby for values of $\Delta v_p \leq 0$ no constriction formation was detected

was present. Such a constriction formation could not be detected in the case of $\Delta v_p = 0$ mm/s.

5 Discussion

Regarding the working hypothesis of this study, it was shown that a constriction formation occurs when the process velocity is higher than the component of the wire velocity in the process direction (cf. Fig. 9). To validate

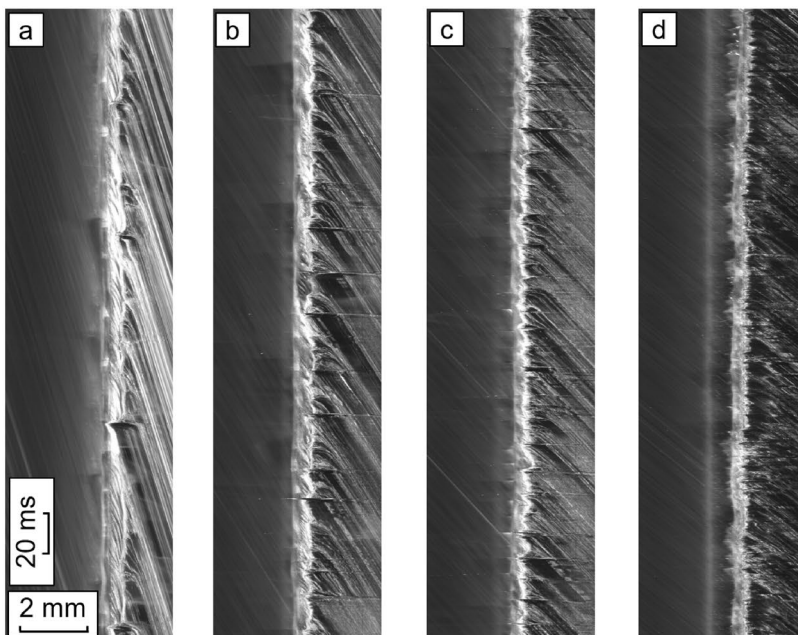


laser	Trumpf TruDisk 12002
base material	DC06 + ZE75/75
filler material	CuSi3Mn1
laser spot diameter	2.4 mm
wire diameter	1.2 mm
wire angle	40 °
energy per wire amount	40 J/mm ³
wire velocity	50 mm/s
laser power	2.26 kW
process velocity	varied

BIAS ID 200450

Mattulat 2020

Fig. 12 Determined blowout event densities for varied Δv_p



laser	Trumpf TruDisk 12002
base material	DC06 + ZE75/75
filler material	CuSi3Mn1
laser spot diameter	2.4 mm
wire diameter	1.2 mm
wire angle	40 °
energy per wire amount	40 J/mm ³
velocity difference Δv_p	0 mm/s

	v_p	v_w
a	19.2 mm/s	25 mm/s
b	38.3 mm/s	50 mm/s
c	57.5 mm/s	75 mm/s
d	76.6 mm/s	100 mm/s

BIAS ID 200451

Mattulat 2020

Fig. 13 Streak images for experiments with different values for the wire velocity but constant $\Delta v_p=0$ mm/s

this statement, the process velocity was varied in order to show that it is not the increase in the process velocity that causes the constriction formation. Here even with increased process velocity a prevention of constriction formation could be achieved by eliminating the velocity difference Δv_p by adjusting the wire velocity (cf. Fig. 15 or also the online resources 1 and 2). Furthermore, the effect of a changing wire position (due to a disturbed melting behavior of the filler wire) was assumed as a possible reason for the constriction formation, but it can be proven that no change in wire position occurred during

the experiments (cf. Fig. 10). Therefore, the resulting relative velocity in the process zone Δv_p is identified as the main cause of the constriction formation. The constriction formation does not occur when the wire velocity in the process direction becomes higher than the process velocity (cf. Fig. 9). The effect that is responsible for the formation of constrictions is the consequently pulling forces from the workpiece on the melt pool of the braze seam and from that on the melting wire due to a too high process velocity or a too low wire velocity, respectively.

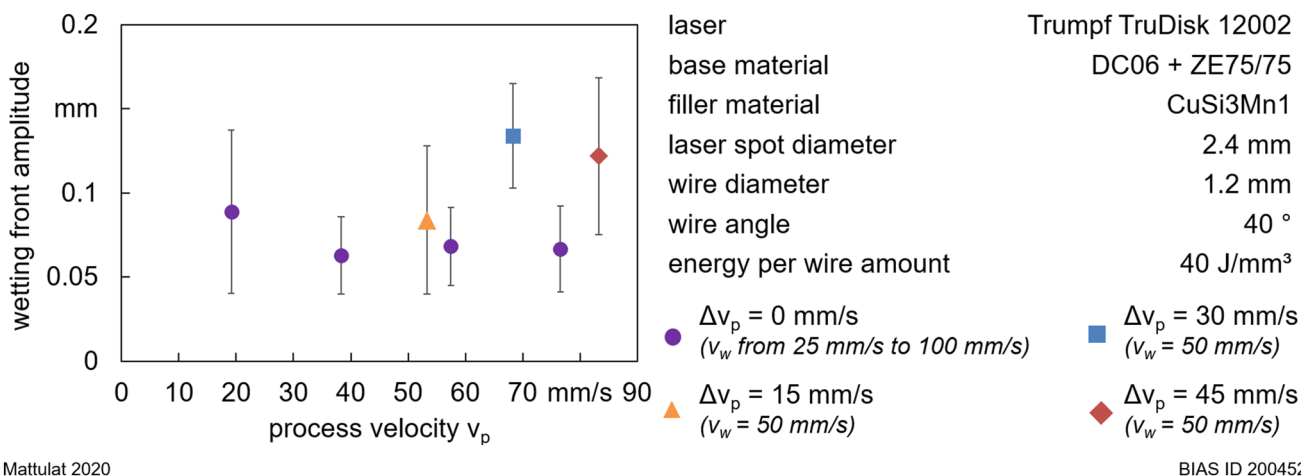


Fig. 14 Comparison of measured wetting front amplitudes for different process velocities and varied velocity differences

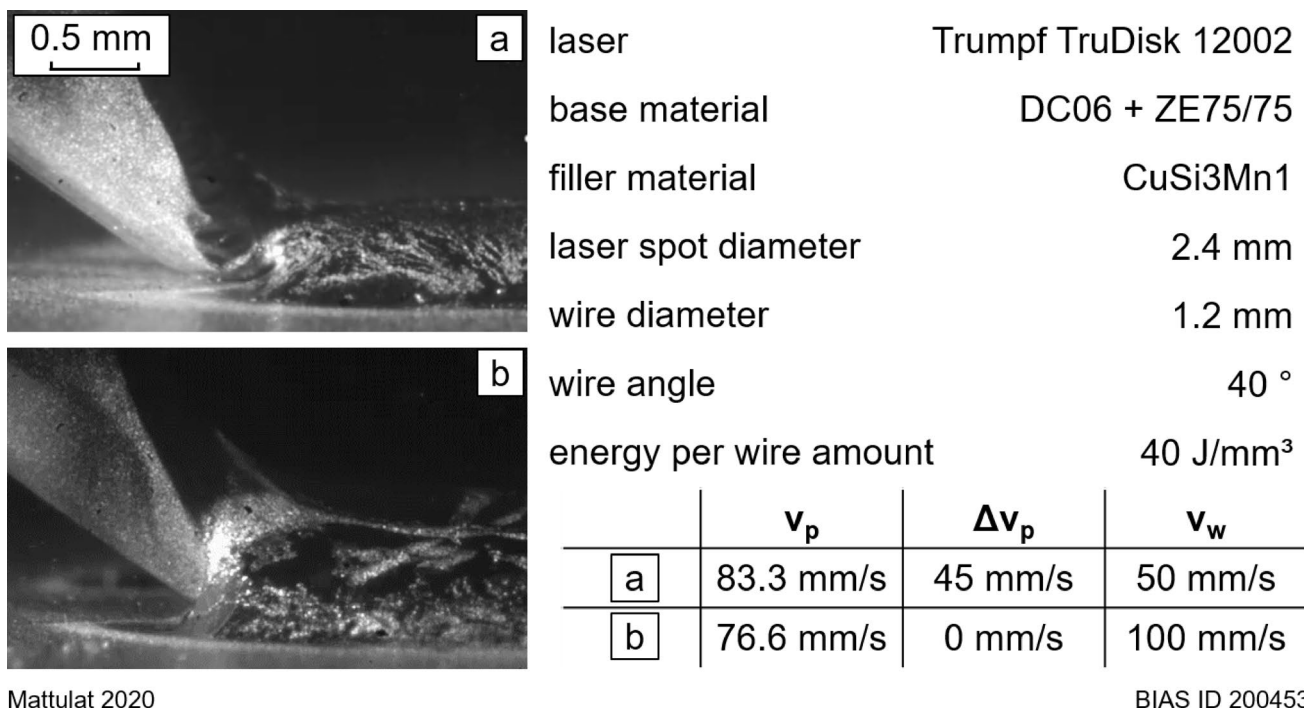


Fig. 15 Direct comparison of the process recordings of two experiments that differed in Δv_p but had comparable values for the process velocity v_p

If the process velocity slightly exceeds the wire velocity in the process direction, a constriction formation occurs that is not stable (cf. Fig. 7 and online resource 1). These constrictions can collapse at irregular intervals, resulting in an increased variation of the wetting front position (cf. Fig. 8) and thus an abrupt and stepwise progressing wetting process. Furthermore, according to Heuberger et al., these constriction collapses can affect the optical seam quality and induce seam edge defects, such as notches [14]. In the

experiments carried out, this regime, with unstable constriction formation and subsequent collapses, was identified between $\Delta v_p = 15$ mm/s and $\Delta v_p = 45$ mm/s (cf. Fig. 8). With a further increase in the velocity difference, the constriction formation stabilizes so that no further collapses of the constrictions occur (cf. Fig. 7 and online resource 3). This results in a more uniform wetting process (cf. Fig. 8). In this second regime, with a low wetting front fluctuation due to the stable constriction formation, the density of blowout

events is, in addition, significantly reduced (cf. Fig. 12). The reason for these blowout events is considered to be the evaporation of low-boiling zinc through the melt pool, as described by Kimura et al. [18]. It is therefore plausible that the permanently open (cf. online resource 3) and elongated (cf. Fig. 11) constrictions at high values of Δv_p support the outgassing of evaporating zinc so that the zinc vapor no longer has to escape through the melt pool or by blowout events.

With regard to a suitable process control for the industrial application of laser brazing, two strategies can be drawn from the presented findings:

1. In order to avoid the formation of constrictions, the relationship between the process velocity and the wire velocity component oriented parallel to the process direction can be adjusted to 0 mm/s, which has been proved to be effective for different process velocities from 19 to 77 mm/s (cf. Figs. 13 and 14). It must be taken into account that the wire volume per seam length then changes. This could possibly be compensated by the wire diameter, although the influences on the wetting behavior and the occurrence of blowout events were not considered in this study.
2. With a focus on achieving high process velocities, and therefore low cycle times in the production process, the objective in process control can be to braze in the supercritical area at a high velocity difference, whereby the constriction formation stabilizes. Hereby, a constant wetting progress as well as the absence of blowout events can be achieved.

6 Conclusion

The following conclusions can be drawn from the investigations:

1. The formation of constrictions in the wetting process during laser brazing is determined by the difference between the process velocity and the component of the wire velocity in the process direction.
2. If the process velocity exceeds the component of the wire velocity in the process direction, the formation of constrictions is observed.
 - a. For slightly higher process velocities, this constriction formation is not stable and the constrictions repetitively collapse resulting in an abrupt propagation of the wetting process.
 - b. With further increases in the velocity difference, the constriction formation is stabilized and the constrictions do not collapse but remain open. This homog-

enizes the wetting progress and reduces the occurrence of blowout events in the area of the wetting front.

Acknowledgements The IGF-Project no.: 19.987 N/DVS-No.: 06.3047 of the “Forschungsvereinigung Schweißen und verwandte Verfahren e.V.” of the German Welding Society (DVS), Aachener Str. 172, 40223 Düsseldorf was funded by the Federal Ministry for Economic Affairs and Energy (BMWi) via the German Federation of Industrial Research Associations (AiF) in accordance with the policy to support the Industrial Collective Research (IGF) on the orders of the German Bundestag. Furthermore, the authors gratefully acknowledge the collaboration with the members of the project affiliated committee regarding the support of knowledge, material, and equipment over the course of the research. The “BIAS ID” numbers are part of the figures and allow the (re)traceability of the results with respect to mandatory documentation required by the funding organization.

Author contributions T. Mattulat and P. Woizeschke contributed to the study conception and design. Material preparation, data collection and analysis were performed by T. Mattulat. The first draft of the manuscript and the visualizations were created by T. Mattulat. The project administration and the review and editing of the manuscript were carried out by P. Woizeschke. T. Mattulat and P. Woizeschke read and approved the final manuscript.

Funding The results were obtained in the course of investigations within the IGF-Project no.: 19.987 N/DVS-No.: 06.3047, which is part of the “Forschungsvereinigung Schweißen und verwandte Verfahren e.V.” of the German Welding Society (DVS), Aachener Str. 172, 40223 Düsseldorf. It was funded by the Federal Ministry for Economic Affairs and Energy (BMWi) via the German Federation of Industrial Research Associations (AiF) in accordance with the policy to support the Industrial Collective Research (IGF) on the orders of the German Bundestag. Open Access funding provided by Projekt DEAL.

Availability of data and material Additional high-speed recordings are supplemented to visualize the constriction formation and the described effects concerning the wetting process.

Code availability There is no supplementary code available.

Compliance with ethical standards

Conflict of interest The authors declare that they have no conflict of interest or competing interests.

Open Access This article is licensed under a Creative Commons Attribution 4.0 International License, which permits use, sharing, adaptation, distribution and reproduction in any medium or format, as long as you give appropriate credit to the original author(s) and the source, provide a link to the Creative Commons licence, and indicate if changes were made. The images or other third party material in this article are included in the article’s Creative Commons licence, unless indicated otherwise in a credit line to the material. If material is not included in the article’s Creative Commons licence and your intended use is not permitted by statutory regulation or exceeds the permitted use, you will need to obtain permission directly from the copyright holder. To view a copy of this licence, visit <http://creativecommons.org/licenses/by/4.0/>.

References

- Schmidt M, Zäh M, Li L et al (2018) Advances in macro-scale laser processing. *CIRP Ann* 67(2):719–742. <https://doi.org/10.1016/j.cirp.2018.05.006>
- Loeffler K, Morris T, Trumpf V (2004) Laser processing. In: Golf V, Ebert F, Niemeyer M, (eds.) Proceedings of the 7th European automotive laser application conference (EALA)
- Milberg J, Trautmann A (2009) Defect-free joining of zinc-coated steels by bifocal hybrid laser welding. *Prod Eng Res Devel* 3(1):9–15. <https://doi.org/10.1007/s11740-008-0140-2>
- Hornig H (2006) Praxis des Laserstrahlhartlötens im Fahrzeugbau. Proceedings of 5th Laser-Anwenderforum
- Husner J, Luft A, Olainek C (2003) Laserlötens im Automobilbau. ThyssenKrupp techforum
- Graudenz M, Heitmanek M (2012) Laser tools in the manufacturing process. *LTJ* 9(4):24–27. <https://doi.org/10.1002/latj.201290049>
- Haldenwanger H-D, Schmid G, Korte M et al (1999) Laserstrahlhartlötens für Karosserieteile in Claas-A-Oberflächenqualität. *Schweißen und Schneiden* 99. *DVS Rep* 204:191–196
- Sander J, Reimann W (2015) Development of a benchmark criteria for the evaluation of optical surface appearance qualities of brazing and welding connections. Proceedings of the 17th European Automotive Laser Applications EALA
- Mattulat T, Kügler H (2020) Investigations on the occurrence of different wetting regimes in laser brazing of zinc-coated steel sheets. *Welding World* 64:449–456. <https://doi.org/10.1007/s40194-019-00843-9>
- Frank S, Ungers M, Rolser R (2011) Coaxial control of aluminum and steel laser brazing processes. *Phys Proc* 12:752–760. <https://doi.org/10.1016/j.phpro.2011.03.094>
- Grimm A, Schmidt M (2009) Possibilities for online process monitoring at laser brazing based on two dimensional detector systems. Proceedings of 28th International Congress on Applications of Laser & Electro-Optics (ICALEO), pp 537–544
- Reimann W (2018) Entwicklung eines Laserstrahl-Lötverfahrens für schmelztauchveredelte Karosseriebauteile. Dissertation. In: Dilger K (ed) Forschungsberichte des Instituts für Füge- und Schweißtechnik, vol 47. Shaker Verlag, Aachen
- Heitmanek M, Dobler M, Graudenz M et al (2014) Laser brazing with beam scanning: experimental and simulative analysis. *Phys Proc* 56:689–698. <https://doi.org/10.1016/j.phpro.2014.08.076>
- Heuberger E, Schmid D, Weberpals J-P et al. (2018) Influence of the brazing speed on the seam characteristics in laser beam brazing of zinc coated steel. Proceedings of the International Congress on Applications of Lasers and Electro-Optics ICALEO, Orlando, USA, Paper #903
- Mattulat T, Woizeschke P (2020) Manipulation of the cyclic wetting process using longitudinal filler wire oscillation in the laser brazing of zinc-coated steel sheets. *Procedia CIRP (Accepted)*
- Gatzen M, Radel T, Thomy C et al (2014) Wetting behavior of eutectic Al–Si droplets on zinc coated steel substrates. *J Mater Process Technol* 214(1):123–131. <https://doi.org/10.1016/j.jmatp.2013.08.005>
- Schmidt M, Otto A, Kägeler C (2008) Analysis of YAG laser lap-welding of zinc coated steel sheets. *CIRP Ann* 57(1):213–216. <https://doi.org/10.1016/j.cirp.2008.03.043>
- Kimura S, Takemura S, Mizutani M et al. (2006) Laser brazing phenomena of galvanized steel and pit formation mechanism. Proceedings of the International Congress on Applications of Lasers and Electro-Optics ICALEO, Orlando, USA, Paper #528

Publisher's Note Springer Nature remains neutral with regard to jurisdictional claims in published maps and institutional affiliations.